AI-Based EMT Dynamic Model of PV Systems

Suman Debnath
Energy Science & Technology Directorate
Oak Ridge National Laboratory
Knoxville, USA
debnaths@ornl.gov

Phani R V Marthi
Energy Science & Technology Directorate
Oak Ridge National Laboratory
Knoxville, USA
marthip@ornl.gov

Qianxue Xia
Energy Science & Technology Directorate
Oak Ridge National Laboratory
Knoxville, USA
xiaq@ornl.gov

***Abstract*—Several electromagnetic transient (EMT) dynamic modeling methods are available to model systems like photovoltaic (PV) plants, wind power plants, variable-speed drives, among others. The methods include: (a) physics-based models and (b) data-driven models. The physics-based dynamic models may include high-fidelity switched system model and average-value model that both require the control algorithms included in the models. However, manufacturers typically prefer to provide black-box models to avoid disclosing proprietary. One of the solutions to prevent disclosing control algorithms is the use of data-driven dynamic EMT models of PV systems. In this paper, data-driven dynamic EMT model based on artificial intelligence (AI) algorithms are presented. The AI algorithms evaluated include convolutional neural networks, recurrent neural networks, and nonlinear auto-regressive exogenous model. Automation in generating data and training these models is also discussed in this paper. The results generated by the best AI algorithms have been observed to be greater than 95% accurate.**

***Index Terms*—PV Plant, AI, Surrogate Model, Automation, EMT**

I. Introduction

In the recent times, there is a recognition to perform electromagnetic transient (EMT) simulations for larger power grids with more detailed equipment models [1], [2]. To simulate power grids with equipments in EMT simulators, EMT simulation models that are either physics-based or data-driven are needed. These models need to be comprehensively tested and the process to generate these models is being standardized (by North American Electric Reliability Corporation [NERC]) for example). Physics-based EMT models of equipment (like high-voltage direct current [HVdc], photovoltaic [PV] power plants, extreme fast electric vehicle chargers [xFC], industrial drives, etc.) can be high-fidelity detailed switched system models [3]–[7], average-value models [7], [8], and other reduced-order models [9]. Data-driven EMT models of equipment can include system identification in transfer functions in frequency domain (linear models) [10], Hammerstein Wiener model (non-linear model) [11], artificial neural network model (non-linear model) [12], polytopic black-box model [13], and a combination of one or more techniques [14]. A review of different data-driven and physics-based models has been performed on microgrids with comparison between different data-driven models shown [15] and on power electronic converters in power grids [7]. Moreover, data-driven EMT models have been used for intelligent predictions to identify bad data read from sensors in power electronics [16].

While the preference is for high-fidelity switched system models in EMT simulations to understand the interactions between equipment (like a PV plant) and power grid, data-driven models may be utilized where it is challenging to get access to high-fidelity switched system model. In this paper, different data-driven artificial intelligence (AI) models are evaluated for modeling a PV system. The AI-based models include convolutional neural networks (CNNs), recurrent neural networks (RNNs), and nonlinear auto-regressive exogenous model (NARX). These AI models are evaluated to identify the algorithms that show promise for data-driven modeling of power electronics systems like PV power plants. Automation in the process to generate these models is also discussed in the paper.

II. PV Power Plant

A typical PV power plant is shown in [4]. The plant consists with a power transformer, distribution lines, distribution transformers, inverters (with their filters), and PV arrays. There are in the range of hundreds of lines, transformers, inverters (with their filters), and PV arrays in a large PV power plant. A PV system comprises of a single distribution transformer that may connect to multiple inverters with their filters in the low voltage side of the transformer.

The control system of the PV power plant typically consists of the power plant controller (PPC) that sends active and reactive power dispatch commands to the inverter controllers and receives information on measured active and reactive power along with voltage and frequency at the terminal of the PV power plant. The inverter controller controls the active and reactive power at the inverter terminals based on the dispatch commands received from PPC and regulates the

Research sponsored by Solar Energy Technologies Office of U.S. Department of Energy. This material is based upon work supported by the U.S. Department of Energy's Office of Energy Efficiency and Renewable Energy (EERE) under the Solar Energy Technologies Office Award Number 36532. The views expressed herein do not necessarily represent the views of the U.S. Department of Energy or the United States Government.

internal variables (like ac-side currents, dc-side current, dc-side voltage, among others).

III. AI Models

Different AI model are evaluated in this section for evaluating the dynamics of a PV system. They include CNN, RNN, and NARX.

A. Training Dataset

The data required in the AI-based models for comparing the different algorithms include the single-phase ac-side voltages at the inverter terminals, the PV power generated, and the corresponding single-phase ac-side currents at the inverter terminals. In this research, this dataset is generated from the simulation in PSCAD of the high-fidelity switched system dynamic EMT model [4] that includes a single PV system that connects to a distribution line. The distribution line connects to a controlled voltage source at the other end. The voltage and frequency of the controlled voltage source are varied to provide data for grid events where voltage and frequency variations are observable. The voltage variation may happen when there are unbalanced line-line faults and three-phase faults in the ac grid. The frequency variation may happen when there is a loss of generation in the ac grid. The sampling frequency considered while generating this dataset is $50\mu s$. This dataset is used to train the AI models and compare their performance.

B. NARX Model

A NARX model consisting of layers processing current and previous time-step inputs and outputs from the model is considered for representing the dynamics of a PV system. The NARX model with two layers is shown in Fig. 1. The model shown in the figure is a series-parallel architecture, with inputs and previous time-step outputs being fed in as inputs to the model. The outcome of the model is the current time-step output. The parameters like number of previous time-step inputs, number of previous time-step outputs, and number of layers can be varied to improve the accuracy of the model.

C. CNN Model

A CNN model consisting of convolutions, dropouts, transpose of convolution, and max pooling is considered for representing the dynamics of a PV system. Each layer consists of multiple neurons with activation functions. An example CNN model is shown in Fig. 2. The activation functions considered are rectified linear unit (RELU) and tanh functions. The parameters like type of layer (convolution, transpose of convolution, max pooling, dropouts, etc.) and its parameters, activation function, number of layers, and number of neurons in each layer can be varied to improve the accuracy of the model

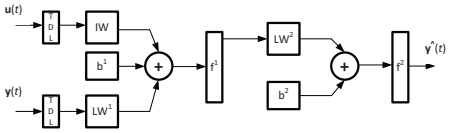

Fig. 1. NARX model.

D. RNN Model

An RNN model consisting of present layers and history layer is considered for representing the dynamics of a PV system. Each layer consists of multiple neurons with activation functions. The history layer uses the data from the previous time-step to update the input to the neuron in the current time-step. An example implementation of the RNN model is shown in Fig. 3. The activation functions considered are RELU and tanh functions. The parameters like number of layers, number of history layers, number of neurons in each layer, and activation function can be varied to improve the accuracy of the model.

E. Training & Comparison

The AI models, CNN and RNN, are trained in Python based on the training dataset. Based on variations in the number of layers from 2 to 4 and the corresponding associated parameters in the CNN model, it was identified that the best results were obtained from a 3-layer model. The 3 layers consist of 50 filters convolution with RELU activation function, 1 filter transpose of convolution with tanh activation function, and max pooling, respectively. There are a total of $1,101$ trainable parameters. Similarly, varying the number of layers from 2 to 3 and the corresponding parameters in the RNN model, it was identified that the best results were obtained from a 2-layer model. The 2 layers consist of 20 neurons with RELU activation function and 1 neuron with tanh activation function, respectively. There are a total of 482 trainable parameters.

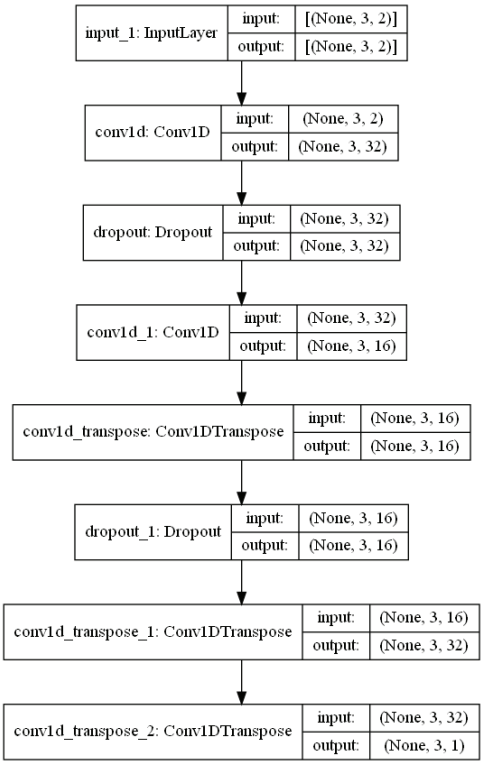

Fig. 2. CNN model.

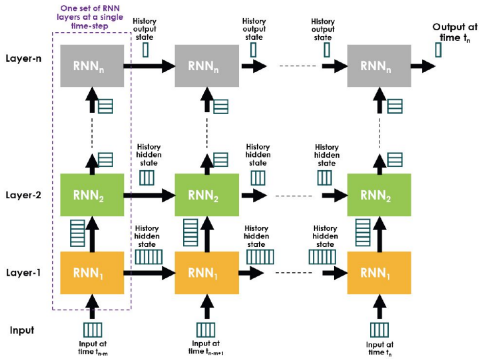

Fig. 3. Typical RNN model.

The NARX model is trained in MATLAB based on the same training dataset. The training yields the best results with 1 previous time-step input, 1 previous time-step output, and 3 layers. However, there were challenges observed with the closed-loop NARX implementation as the validation test results were not very similar to the validation datasets. While open-loop NARX in estimation problems have shown good replication (e.g., [16]), closed-loop NARX that can be used in EMT dynamic model development appears to have challenges with initialization. In estimation problems, the historical measured data can be used as previous time-step output that are fed as inputs to the NARX model in open-loop. In the closed-loop NARX model, the output of the NARX model from the previous time-step is fed as an input. This makes it more challenging to achieve convergence and introduces initialization problems.

From the trained models, it has been observed that the RNN model imposes the least computational burden while providing very good similarity to the test data.

IV. Automation of Generating & Testing AI-Based Model

Based on the comparison discussed in the previous section, in this section, the RNN algorithm is considered to develop the EMT dynamic model of a PV system. The overview of the automation performed to generate the RNN-based model and integrate with the EMT model of the rest of the power grid is automated and can be implemented by a single click of a Python script.

A. Data Generation

The dataset needed to train the RNN model is generated from the simulation in PSCAD of the same high-fidelity switched system EMT dynamic model explained in Section III-A. In additiona to varying the voltage magnitude and frequency of the controlled voltage source, the PV power generation is varied at each voltage and frequency to generate a comprehensive dataset. Another important parameter in the dataset generation is the sampling frequency required for the dataset.

The dataset generation process has been fine-tuned after multiple iterations of the type of data, sampling frequency of data captured, and operating conditions at which data is generated have been tried and tested. Finally, the data required to train the RNN model include the three-phase ac-side voltages at the PV system terminals, the PV active and reactive powers generated, and the three-phase ac-side currents at the PV system terminals. The dataset finally generated is sampled at $50\mu s$. This dataset is generated at 7 different PV power generation set points and at each generation set point, 3 different distribution grid voltage magnitude and 2 different distribution voltage frequencies are considered. A total of $140,000$ data points is generated.

The process to generate the dataset is automated through Python scripting and the generated data is processed to inputs and outputs needed to train each RNN model.

B. Training

Once the dataset is generated from PSCAD, it is used to train an RNN model in Python. The number of layers, number of neurons in each layer (and correspondingly the weights and biases), type of activation function, the number of history layers, and input-output combinations are the parameters available in the RNN model to tune. Multiple training runs are completed on the generated dataset to fine-tune the parameters that result in the best fit of the available data to the RNN model.

Initially, a single RNN model is considered for a PV system. The single RNN model is trained using input data of three-phase ac-side voltages at inverter terminals and PV active and reactive powers generated. The output data is the three-phase ac-side currents. The RNN model generated uses three layers, 10 neurons in the hidden layer and 3 neurons in the output layer, RELU and tanh activation functions in the hidden layer and output layer, respectively, and 1 history layer. However, the output did not match well once the training was completed. Hence, the output data was reduced to single-phase ac-side current, while the input data remained the same to train a single RNN model. That is, a total of 3 RNN models is required to generate the three-phase ac-side currents as outputs. The RNN model's parameters were varied and finally, a 3-layer RNN model with 10, 3, and 1 neurons in the multiple hidden and output layers produced the best fit to the available dataset. The RNN model uses RELU, tanh, and tanh activation functions, respectively, in the 3 layers. It also uses 1 history layer.

The process to train the RNN model, extract parameters (gains, biases) from the trained RNN model, and store the extracted parameters in the file system is completely automated in Python.

C. C Code Development

A general-purpose RNN model is developed in C code that takes gains and biases as inputs. A sample RNN model is shown in Fig. 3 to indicate the structure of the model that is implemented in C code. The code implemented in C represents only one time-step (or, equivalently, one set of RNN layers in Fig. 3). This C code is callable from PSCAD with gains and biases sent from PSCAD.

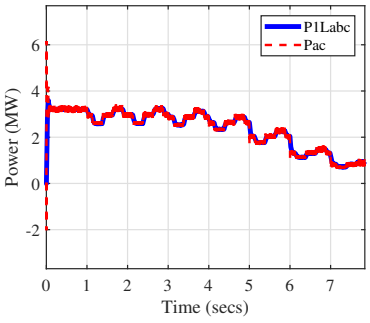

(a)

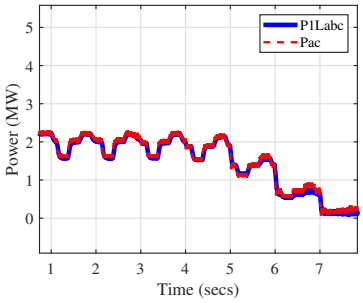

(b)

Fig. 4. Comparison of the active power from the PV system through simulation of RNN-based EMT dynamic model (Pac) and high-fidelity switched system EMT dynamic model (P1Labc) for two different PV systems: (a) PV system-1, (b) PV system-2.

D. PSCAD-C AI-Based Model

The RNN models representing a single PV system are integrated with the rest of the circuit in PSCAD. The RNN models feed the three-phase currents to the circuit and take in the measured three-phase voltages from the circuit along with the active/reactive power references from the PPC as inputs. This interaction between the RNN model in C code and the circuit that the RNN model connects to is implemented in a Fortran script within PSCAD.

The Fortran script in PSCAD, first, calls a C code that extracts the parameters of the trained RNN models for the three phases of a PV system from the file system. The measured three-phase voltages from the PSCAD circuit and the active/reactive power references from the PPC are sent to the Fortran scripts at inputs that can be used in the three RNN models. These inputs are normalized and biases are removed. Then, the Fortran script calls the three RNN models in C codes and passes the inputs to generate the single-phase ac-side current from each RNN model. The generated three-phase ac-side currents from the three RNN models are fed from the Fortran script to the circuit implemented in PSCAD.

V. Integration of AI-based model to PV distribution grid

The AI-based PV (photovoltaic) plant model was integrated with the developed distribution grid model in PSCAD, and the response of the PV plant, along with the current power plant controller, was analyzed.

The training process for the advanced photovoltaic (PV) model of the generic PV plant has faced challenges in fully capturing the transient behavior of the high-fidelity PV model. As a result, when integrating the AI-based PV model into the distribution grid, the system becomes unstable. This instability may arise from a mismatch in dynamics. The distribution grid model, being a damped system, may have a slower response compared to the AI-based model, which is undamped and respond instantly to changes in its input. The damping in the distribution grid model may cause it to exhibit oscillatory behavior, especially if it is underdamped. If the AI-based PV model does not account for this behavior and reacts only to the instantaneous value of its input, it might generate outputs that exacerbate the oscillations, leading to instability. Additionally, since the integrated PV model is AI-based and hasn't been trained with a dataset coming from the complete PV plant system with distribution grid model, it might not be able to handle the dynamics introduced by the damping in the distribution grid model when they are connected.

Several possible solutions to address the instability have been proposed, including: tuning the damping in the distribution grid model; designing extra control for integrating the AI-based PV model with the distribution grid model; and modifying the AI-based PV model. The simplest method, which has been adopted, involves incorporating some form of damping or feedback control into the AI-based PV model to help stabilize the loop. Thus, additional capacitance was incorporated at the bus of each PV cell location. A thorough investigation was conducted by sweeping the added capacitance at each location and identifying the minimum additional capacitance required to minimize the total reactive power for the PV plant. By leveraging this minimum additional capacitance, the advanced generic PV model can achieve stability and reliable performance. The additional capacitance may affect the reactive power of the PV plant, but the active power command can still be perfectly tracked.

VI. Simulation Results

A. Comparison between RNN-based EMT dynamic model and the high-fidelity switched system EMT dynamic model for the same PV systems

For two different real PV systems in the field, a comparison between the simulation results of the RNN-based EMT dynamic model and the high-fidelity switched system EMT dynamic model for the same PV systems is shown in Fig. 4. From the figure, it may be observed that the simulation results from the RNN-based EMT dynamic model closely match the simulation results from the high-fidelity switched system EMT dynamic model for both the PV systems. The automation in generating and testing the RNN-based EMT dynamic model is helpful when different PV systems are being considered. From the comparison, the accuracy observed in the RNN-based EMT dynamic model is greater than 95%. The speed-up in simulation of RNN-based EMT dynamic model of the

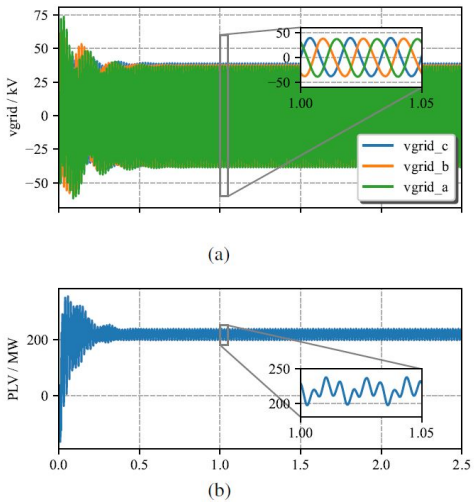

Fig. 5. Simulation results for the integrated AI-based PV system with distribution grid: (a) Grid Lower voltage side voltage, (b) Grid lower voltage side active power.

PV system is compared with the simulation of the baseline EMT dynamic model of the same PV system in PSCAD. The baseline EMT dynamic model of the PV system utilizes the library components in PSCAD. A speed-up of the order of up to 100x is observed in a single PV system.

B. Integrate the AI-based PV system with distribution grid

The simulation results for the complete PV plant with power transformer (230kV/34.5kV), distribution grid, and AI-based PV system is presented in Fig. 5. The dispatch command for the active power is set at 200MW. As illustrated in Fig. 5 (a), the grid-size voltage at the lower side of the power transformer exhibits stable results with the integration of the additional capacitance. Additionally, Fig. 5 (b) demonstrates that the active power consistently tracks its reference value.

VII. Conclusions

In this paper, three different AI-based models (RNN, CNN, and NARX) were developed to represent the EMT dynamics of PV systems. Upon evaluation under different operating conditions, it has been identified that the RNN-based models present the best representation of the EMT dynamic of a PV system. A fully automated process to develop the RNN-based EMT dynamic model of PV systems and test them is presented in the paper. The simulation results from the RNN-based EMT dynamic models of two different PV systems, as compared to the corresponding high-fidelity switched system EMT dynamic model of the PV system, has shown a high degree of accuracy and a speed-up of up to 100x.

Acknowledgment

Authors would like to thank Kemal Celik for overseeing the project developments and providing guidance.

References

[1] "Odessa Disturbance Texas Events: May 9, 2021 and June 26, 2021," *North American Electric Reliability Corporation*, September 2021.

[2] S. Debnath, M. Elizondo, Y. Liu, P. Marthi, W. Du, S. Marti, and Q. Huang, "High penetration power electronics grid: Modeling and simulation gap analysis," 8 2020.

[3] Q. Xia, S. Debnath, P. R. V. Marthi, S. Marti, and M. Saeedifard, "High-fidelity models and fast emt simulation algorithms for isolated multi-port autonomous reconfigurable solar power plant (mars)," in *2021 IEEE 12th International Symposium on Power Electronics for Distributed Generation Systems (PEDG)*, 2021, pp. 1–7.

[4] J. Choi and S. Debnath, "Electromagnetic transient (emt) simulation algorithm for evaluation of photovoltaic (pv) generation systems," in *2021 IEEE Kansas Power and Energy Conference (KPEC)*, 2021, pp. 1–6.

[5] S. Debnath and J. Choi, "Electromagnetic transient (emt) simulation algorithms for evaluation of large-scale extreme fast charging systems (t & d models)," *IEEE Transactions on Power Systems*, pp. 1–11, 2022.

[6] N. Guo and W. Liu, "Power electronic switching models for numerical simulations of power system electromagnetic transient," in *2019 IEEE 8th International Conference on Advanced Power System Automation and Protection (APAP)*, 2019, pp. 1026–1030.

[7] C. Shah, J. D. Vasquez-Plaza, D. D. Campo-Ossa, J. F. Patarroyo-Montenegro, N. Guruwacharya, N. Bhujel, R. D. Trevizan, F. A. Rengifo, M. Shirazi, R. Tonkoski, R. Wies, T. M. Hansen, and P. Cicilio, "Review of dynamic and transient modeling of power electronic converters for converter dominated power systems," *IEEE Access*, vol. 9, pp. 82 094–82 117, 2021.

[8] X. Yue, X. Wang, and F. Blaabjerg, "Review of small-signal modeling methods including frequency-coupling dynamics of power converters," *IEEE Transactions on Power Electronics*, vol. 34, no. 4, pp. 3313–3328, 2019.

[9] Y. Liao and X. Wang, "Small-signal modeling of ac power electronic systems: Critical review and unified modeling," *IEEE Open Journal of Power Electronics*, vol. 2, pp. 424–439, 2021.

[10] N. Guruwacharya, N. Bhujel, U. Tamrakar, M. Rauniyar, S. Subedi, S. E. Berg, T. M. Hansen, and R. Tonkoski, "Data-driven power electronic converter modeling for low inertia power system dynamic studies," in *2020 IEEE Power Energy Society General Meeting (PESGM)*, 2020, pp. 1–5.

[11] M. E. A. Alqahtani, M. Alsaffar and B. Alajmi, "Data-driven photovoltaic system modeling based on nonlinear system identification," *International Journal Photoenergy*, 2016.

[12] H. Abbood and A. Benigni, "Data-driven modeling of a commercial photovoltaic microinverter," in *Modelling and Simulation in Engineering*, 2018, pp. 1–11.

[13] L. Arnedo, D. Boroyevich, R. Burgos, and F. Wang, "Polytopic black-box modeling of dc-dc converters," in *2008 IEEE Power Electronics Specialists Conference*, 2008, pp. 1015–1021.

[14] V. Valdivia, A. Lázaro, A. Barrado, P. Zumel, C. Fernández, and M. Sanz, "Black-box modeling of three phase voltage source inverters based on transient response analysis," in *2010 Twenty-Fifth Annual IEEE Applied Power Electronics Conference and Exposition (APEC)*, 2010, pp. 1279–1286.

[15] A. Francés, R. Asensi, O. García, R. Prieto, and J. Uceda, "Modeling electronic power converters in smart dc microgrids—an overview," *IEEE Transactions on Smart Grid*, vol. 9, no. 6, pp. 6274–6287, 2018.

[16] S. Debnath, S. Kulkarni, and C. Schuman, "Intelligent prediction of states in multi-port autonomous reconfigurable solar power plant (mars)," in *2021 IEEE Energy Conversion Congress and Exposition (ECCE)*, 2021, pp. 1339–1346.